Toward Image-Guided Partial Nephrectomy with the da Vinci Robot: Exploring Surface Acquisition Methods for Intraoperative Re-Registration

James M. Ferguson[*,1,5], Leon Y. Cai[*,2,5], Alexander Reed[4,5], Michael Siebold[4,5], Smita De[3,5], S. Duke Herrell III[1,3,5], and Robert J. Webster III[1,3,4,5]

[1]Vanderbilt University, Department for Mechanical Engineering, Nashville, TN, USA
[2]Vanderbilt University, School of Medicine, Nashville, TN, USA
[3]Vanderbilt University Medical Center, Department of Urologic Surgery, Nashville, TN, USA
[4]Vanderbilt University, Department of Electrical Engineering and Computer Science, Nashville, TN, USA
[5]Vanderbilt Institute for Surgery and Engineering, Nashville, TN, USA
[*]Shared First Authorship

ABSTRACT

Our overarching goal is to facilitate wider adoption of robot-assisted partial nephrectomy through image-guidance, which can enable a surgeon to visualize subsurface features and instrument locations in real time intraoperatively. This is motivated by the observation that while there are compelling lifelong health benefits of partial nephrectomy, radical nephrectomy remains an overused surgical approach for many kidney cancers. Image-guidance may facilitate wider adoption of the procedure because it has the potential to increase surgeons' confidence in efficiently and safely exposing critical structures as well as achieving negative margins with maximal benign tissue sparing, particularly in a minimally invasive setting. To maintain the accuracy of image-guidance during the procedure as the kidney moves, periodic re-registration of medical image data to kidney anatomy is necessary. In this paper, we evaluate three registration approaches for the da Vinci Surgical System that have the potential to enable real-time updates to the display of segmented preoperative images within its console. Specifically, we compare the use of surface ink fiducials triangulated from stereo endoscope images, point clouds obtained without fiducials using a stereoscopic depth mapping algorithm, and points obtained by lightly tracing the da Vinci tool tip over the kidney surface. We compare and contrast the three approaches from both an accuracy and a workflow perspective.

Keywords: da Vinci Robot, Kidney Surgery, Image-Guided Procedures, Registration, Surface Acquisition

1. INTRODUCTION

Surgeons who operate with the da Vinci Surgical System (Intuitive Surgical, Inc., Sunnyvale, CA) currently cannot visualize critical spatial information from preoperative images in real time during a surgery. Instead, they must remember anatomical spatial relationships from previously viewed pre-operative medical images, and mentally estimate the correspondence of image space and the surgical field. A desire for real-time availability of such imaging has motivated prior work aimed to augment the da Vinci Surgical System with image-guidance.[1] For example, Leven et al.[2] integrated laparoscopic ultrasound into the da Vinci Surgeon Console with a focusing application of liver surgery. Another example is the work of Mohareri et al.,[3] who incorporated transrectal ultrasound into the Surgeon Console with registered MRI images to assist in radical prostatectomy. Recently, there has been interest in applying image-guidance specifically for robotic partial nephrectomy, which is our target application in this paper. This is motivated by the high prevalence (63,390 new cases/year) and mortality

Further author information (Send correspondence to J.M.F.):
J.M.F.: E-mail: james.m.ferguson@vanderbilt.edu, Telephone: (615) 557-2279
L.Y.C.: E-mail: leon.y.cai@vanderbilt.edu, Telephone: (614) 719-9355

(13,860 deaths/year) of kidney cancer[4] and the importance of preserving renal function through partial, rather than radical, nephrectomy in appropriate cases.[5,6] Despite the well-established, lifelong benefits for the patient (preserving maximal kidney function), partial nephrectomy is currently underutilized due to the challenge of accomplishing it in a minimally invasive setting. Surgeons instead too often opt for minimally invasive radical nephrectomy.[7]

Based on this compelling clinical motivation, several research groups have worked toward enabling image-guidance within the da Vinci's Surgeon Console as a way to facilitate wider use of robotic partial nephrectomy. Kwartowitz et al.[8] explored using the da Vinci robot as a localizer in image-guidance. Herrell et al.[9] used point-based registration to display 2D CT slices of phantoms in the Surgeon Console to guide resection. Benincasa et al.[10] performed a thorough study (outside the context of the da Vinci) on surface point acquisition exploring how much of the kidney surface (and which areas) are needed to obtain an accurate surface registration. Altamar et al.[11] registered real kidneys to medical images using the da Vinci as a localizer with a surface tracing technique and explored deformation effects as the kidney loses fluid during incision. Pratt et al.[12] incorporated a semi-transparent image overlay into the surgeon's endoscope view using a two-stage, semi-automated registration method in which translation was defined automatically and orientation was set manually by the operating physician. Su et al.[13] used a manual registration method followed by a semi-automated re-registration approach using features detected in the da Vinci's stereo endoscope. After initial visual alignment, manually selected anchor points were tracked by the endoscope to maintain alignment during the overlay of semi-transparent 3D models. Hamarneh et al.[14] conceptually described the various steps needed for image-guided robotic partial nephrectomy performing preliminary, endoscope-based registrations without including robot encoder information or analyzing system accuracy. Schneider et al.[15] proposed the use of a "pick-up" ultrasound transducer inserted during the nephrectomy procedure. This device was grasped by the da Vinci's tool and used to map the vasculature surfaces within the kidney for registration. Hughes-Hallett et al.[16] provide a useful review of registration techniques for the partial nephrectomy procedure.

These promising studies represent steps toward future systems that will account for real-time tissue deformation modeling,[11] topological changes involved in tumor resection,[17,18] gross respiratory and patient motion,[17] and changes to perfusion during partial nephrectomy.[1] Accounting for all of these transient effects in an Image-Guidance System (IGS) will require real-time re-registration of the kidney during the surgical procedure. To address this, in this paper, we explore three methods of organ surface acquisition that could potentially be used for intraoperative re-registration in an IGS for the da Vinci Si Surgical System.

2. SYSTEM CALIBRATION

In our image-guided surgical robotic system, the da Vinci Si Patient Side Manipulator (PSM) tool tips will be tracked using encoder values within the robot arm during surgery and their locations projected onto preoperative, segmented 3D medical image data to guide surgeons during a procedure. They will also be used for registration (via lightly tracing over the surface of the kidney), and compared to endoscope-based registration methods. In all of these approaches, tool tip locations must be known as accurately as possible. To enhance accuracy, we apply a well-known robotic calibration process.[19] Robot calibration involves making minor adjustments to kinematic model parameters to account for factors like manufacturing tolerances and other sources of error to increase model accuracy. After calibrating the da Vinci's PSM instruments, we also calibrated the Endoscopic Camera Manipulator's (ECM) stereo pair which we use to collect surface points through stereoscopic triangulation. A simplified illustration of the da Vinci's manipulator arms can be seen in Fig. 1.

The figure illustrates that each of the da Vinci's manipulator arms have two sets of joints: active (motorized) joints that are actuated under direct physician control and passive (non-motorized) setup joints that are moved infrequently during surgery and serve mainly to position the bases of the active portions of each arm near the patient. These setup joints cannot move on their own and incorporate electronically controlled brakes to lock their positions after the active joints are appropriately positioned.

While all joints are encoded, the encoding of the setup joints has been viewed in the past as less accurate than that of the active joints.[8] It is also worth noting that instrument tip accuracy is in general more sensitive to small angular encoding errors in base joints than in more distal joints. To account for this, we follow an

approach similar to that of Kwartowitz et al.,[8] and attach base coordinate frames at the beginning of the active joints in each arm (see Fig. 1). Part of our calibration procedure is identifying the transformations between these base frames.

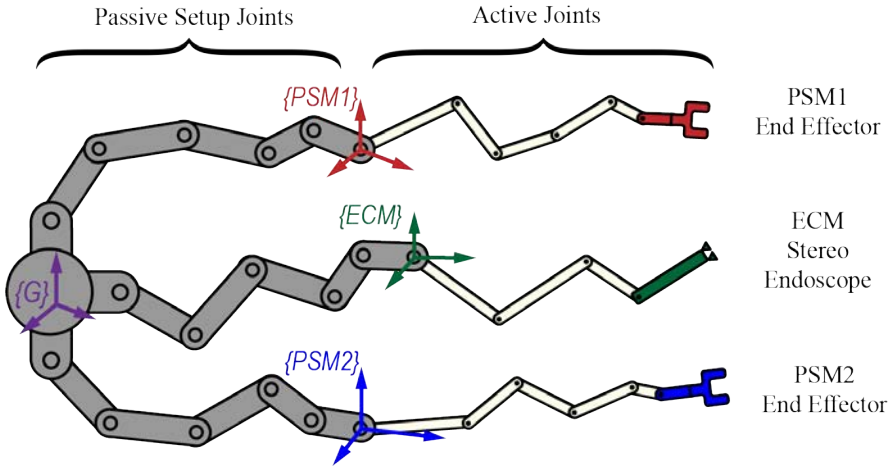

Figure 1. Simplified conceptual illustration of the da Vinci Si manipulator arms as viewed from above illustrating the groups of active and passive joints that comprise each arm, as well as the coordinate frames we attach at the bases of the active portions of each arm.

The da Vinci Surgical System is equipped with a stereo endoscope used to display the surgical scene within the Surgeon Console's 3D display. To calibrate the endoscope for spatial data acquisition, we acquired 30 image pairs of a 7 row by 10 column checkerboard (54 intersections with side length 9.14 mm) all from different ECM poses. MATLAB's stereo camera calibration toolbox[20] was used to calibrate each camera's intrinsic parameters as well as the extrinsic parameters of the stereo pair. This process, and all of our subsequent experiments in this paper, were performed at fixed endoscope zoom and focus settings as to ensure constant camera parameters.

Fiducial Localization Error (FLE) is a measure of a localizer's accuracy in locating spatial data points during image-guidance.[21] To quantify an FLE for the da Vinci's stereo endoscope, we first acquired 10 additional image pairs of the checkerboard pattern. The triangulated checkerboard intersections extracted from these images were point-registered to the known checkerboard dimensions. The FLE components for the stereo endoscope were taken as the differences between the localized points and the known checkerboard dimensions following coregistration. A Quantile-Quantile (QQ) plot was used to characterize the FLE distribution (as was utilized by Kwartowitz et al[22]). The quantiles of the measured FLE data were plotted against the quantiles of a Maxwell-Boltzman distribution (a 3D normal distribution with zero mean). The correlation coefficient ($r = 0.944$) in the QQ plot indicated that the FLE measured for the stereo endoscope was decently modeled by the chosen distribution. The mean and standard deviation of the FLE magnitudes are shown in Table 1.

A similar analysis was performed for each of the PSMs to characterize their respective FLEs. Throughout these experiments, we used the DeBakey Forceps instrument for PSM1 (the "right hand" of the operator) and the Black Diamond Micro Forceps for PSM2 (the "left hand"). With each instrument tip, we carefully probed the 54 intersection points of a larger checkerboard pattern (side length 13.73 mm). When a point in the grid was touched, the robot's encoder values were recorded and used in our forward kinematic model to localize the 3D points. The larger checkerboard pattern was chosen in this case in order to reduce the relative effects of measurement noise, but during calibration of the endoscope, the small checkerboard was chosen to fit into the cameras' fields of view. The probed checkerboard points were registered to the known checkerboard dimensions for each PSM. The FLE components for the PSMs were taken as the registration error of the point-sets as before for the ECM. The PSM FLEs also closely correlated with a Maxwell-Boltzmann distribution meaning that they were indeed normally distributed. The mean and standard deviation of the magnitudes are reported in Table 1.

As mentioned before, the accuracy of the da Vinci manipulators' kinematic models can be enhanced by a calibration procedure. Denavit-Hartenberg (DH) parameters describe the geometry of a serial robot (e.g. the lengths of the robot's linkages, and other similar parameters that are subject to manufacturing tolerances) and

are used in our forward kinematic model for tool tip localization with the PSMs. In the previous procedure characterizing the PSMs' FLE, we used the nominal DH parameters provided with the Intuitive Surgical[23] Application Programming Interface (API).

To calibrate these DH parameters for our particular robot and instruments, we used the larger of the two previously mentioned checkerboard patterns to define a set of points with known geometric relationships and probed them with the da Vinci tool tips. Calibration was performed by optimizing the DH parameters to minimize the difference between the localized grid points and their known dimensions after registration, a standard procedure for robot manipulators (see e.g. Khalil et al.[19]).

Next, the procedure to determine FLE for the PSMs was repeated using independent data sets to characterize reduction in FLE after calibration. We tested how the FLE distribution changed when using the calibrated parameters using a right-sided, one-tailed Wilcoxon signed-rank test.[24] The results of these experiments can be seen in Table 1. The calibrated PSM DH parameters were used in all subsequent experiments in this paper.

Table 1. The FLE for each of the da Vinci manipulators (mean ± standard deviation, mm). The configuration of the setup joints was varied to create the three different Arm Setup configurations listed on the table.

		Arm Setup 1	**Arm Setup 2**	**Arm Setup 3**
PSM1	*Default Model Parameters*	1.08 ± 0.62	1.34 ± 0.58	1.89 ± 0.88
	Calibrated Model Parameters	0.88 ± 0.48	1.17 ± 0.61	1.58 ± 0.84
	Calibration p-value	< 0.01	< 0.01	< 0.01
PSM2	*Default Model Parameters*	1.06 ± 0.53	1.50 ± 0.91	1.78 ± 1.03
	Calibrated Model Parameters	1.00 ± 0.47	1.22 ± 0.76	1.51 ± 1.01
	Calibration p-value	0.33	< 0.01	< 0.01
ECM		0.88 ± 0.58	1.78 ± 1.03	1.59 ± 0.98

Finally, we determine the transformations between the base coordinate frames of the active joints after the passive joints have been positioned and locked. To accomplish this, we probed the intersections of a single fixed checkerboard with each PSM and also triangulated the same point-set with the stereo endoscope. Performing a point-based registration on these point-sets yields the relative transformations of the base frames of each manipulator's active joints.

3. SURFACE ACQUISITION METHODS FOR REGISTRATION

Registration of soft tissues for image-guidance is typically accomplished by matching surface points on the organ collected in the operating room to surfaces segmented from preoperative medical images. We compare three potential methods of intraoperative kidney surface acquisition using our calibrated system for this purpose: (1) using the PSM instruments to lightly trace the kidney surface to digitize a set of points as was performed by Altamar et al.,[11] (2) the use of ink fiducial markers triangulated from stereo endoscope images as proposed by Glisson et al.,[25] and (3) surface points extracted from stereo endoscope images without fiducials using a stereoscopic feature matching algorithm[26] as proposed by Vagvolgyi et al.[27] and Hamarneh et al.[14] These three methods of surface acquisition considered for partial nephrectomy surgery are depicted in Figure 2.

For our registration experiments, we first segmented CT images of a human kidney using the open-source 3D Slicer image segmentation software.[29] These segmentations were used to 3D print (layer thickness 0.13 mm) a 1:1 scale model in hard plastic (Fig 3) to maintain a well-defined and repeatable phantom for surface acquisition. We marked the model with 16 green ink dots in arbitrary locations to serve as camera fiducials for endoscope triangulation and then secured three red pinheads into the surface to serve as target fiducials for error evaluation. Similar ink marks could be made and used in vivo with a surgical ink marker, though the red pins would not be used in a practical clinical system and are included here purely for accuracy assessment.

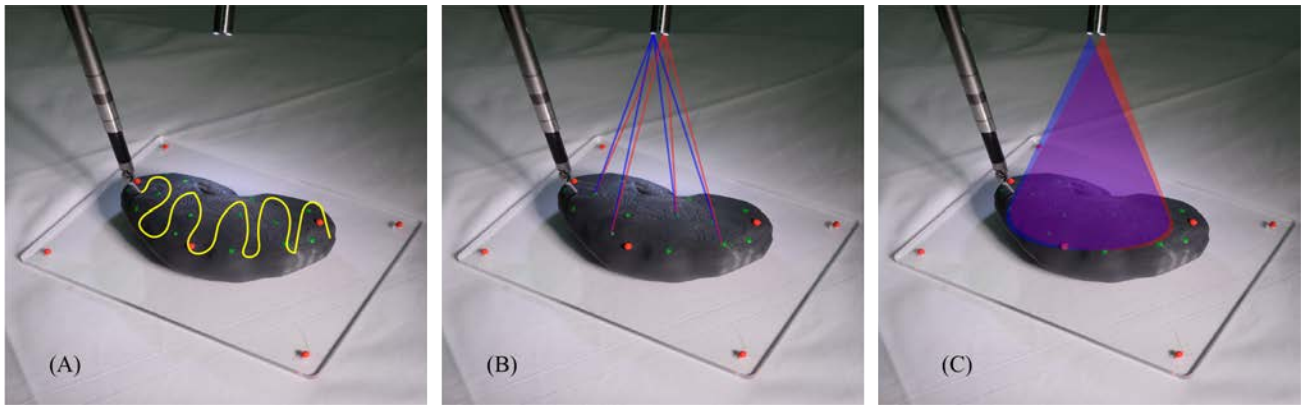

Figure 2. The three methods compared in this paper for organ surface point acquisition enabling registration of CT images to the da Vinci system: (A) Surface tracing with the da Vinci's instrument tool tip. (B) Stereoscopic triangulation of ink fiducial markers on surface anatomy using endoscope images. (C) Point cloud acquisition (surface reconstruction) from endoscope images (without fiducials) using a stereo matching algorithm.[28]

To acquire the model surface and target fiducial locations in image space, we CT scanned our printed model with the xCAT ENT Scanner (Xoran Technologies LLC, Ann Arbor, MI) using a section thickness of 0.5 mm. From these scans, the phantom surface and the target fiducials (i.e. red pinheads) were segmented. After segmentation, we smoothed and re-meshed the model surface with a uniform 0.1 mm distance between mesh vertices using MeshLab, an open-source 3D mesh processing application.[30] This produced a set of 7.1 million points defining the image surface for registration. The centroid coordinates for each of the segmented fiducial targets were also identified to define the target locations in image space. The target coordinates were not used in subsequent registrations. Rather, they were used in computing target registration error after surface registrations were performed.

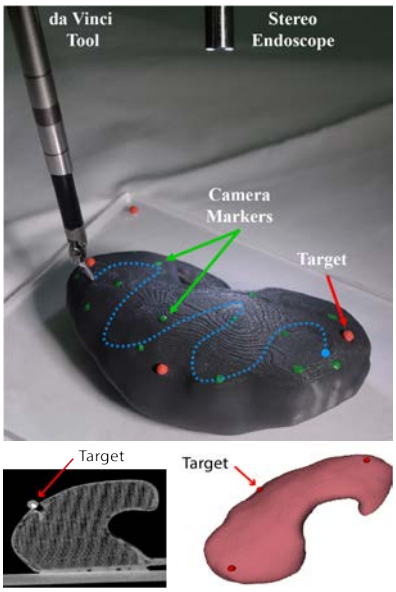

Figure 3. Top: Experimental setup for measurement of target registration error for each of the three surface acquisition methods. Bottom: CT scan of rigid phantom with segmented surface and targets.

During the surface tracing approach (Fig. 2A), the surgeon traces over the surface of the kidney lightly with the PSM tool tip while joint values are recorded at each instant in time using the Application Programming Interface (API) from Intuitive Surgical Inc.[23] With the joint data, the calibrated forward kinematic model is used to compute the tool tip position of the PSM at each point in time as it traces over the surface. The segmented kidney surface in image space is then registered to the array of physical surface points obtained in this manner.

In our registration experiments, after acquiring a set of approximately 2,000 points in this way (a 30 second process), we localized the target fiducials by probing them with the PSM tool tip. When probing the red pinhead targets, to accommodate the 4 mm diameter of the red spheres, we left the jaws of the tool slightly opened and lightly pinched the spherical target fiducial with the tip of the PSM instrument at its midline. Our model predicts the location of the instrument tip as the mid point between the two jaws, meaning that the kinematic point representing the tool tip location is approximately coincident with the center of the spherical target fiducial when it is pinched by the tool tip.

The two other methods of surface acquisition we consider rely on the da Vinci's stereo endoscope. After camera calibration, we triangulate corresponding green ink fiducials as shown in Fig. 2B. For this process, the pixel coordinates of the markers are obtained by color thresholding the stereo images in HSV color space and using the k-means clustering algorithm on each image. The corresponding pixel centroids are then used in stereo triangulation to define a set of surface points for registration. In our experiments, after localization of the green

ink fiducials, the three red target fiducials were triangulated in a similar way to measure target registration error.

The third and final approach we explored for surface acquisition was a fiducial-less depth mapping method (stereo reconstruction) applied to endoscope images acquired from the da Vinci system (Fig. 2C). We use a semi-global stereo matching algorithm[26] (implemented in the MATLAB Computer Vision toolbox) to detect and match features in each of the two endoscope images. A disparity (depth) map is generated from the set of corresponding features. This represents the image depth at a variety of different pixel locations. Using this map, a dense 3D point cloud is produced for use in surface registration. In our experiments, 1,000 feature points were automatically detected, matched, and triangulated. The red target fiducials were acquired with the HSV thresholding method described previously and used to measure target registration error at these points.

Surface point acquisitions were obtained with each of the three methods described above for three separate setup joint configurations. The configurations used were selected arbitrarily, subject to the constraints that they substantially differed from one another spatially and also that they be judged by a physician (participating in these experiments) to be feasible for partial nephrectomy. For each of these setup joint configurations, the full calibration process was performed (see Section 2). Surface data was then acquired five times for each Arm Setup configuration, for each of the three surface acquisition methods under consideration (Figure 2).

A globally-optimal version of Iterative Closest Point (ICP) registration called GoICP (developed by Yang et al.[31]) was then used with each point-set to register image space to physical space. The GoICP algorithm employs a nested Branch and Bound search to guarantee global optimality over the entire domain of $SE(3)$ (the group that describes rigid motion) without requiring excessive computation. A main advantage of GoICP is that no initial guess is needed to initialize the registration procedure. In addition, the algorithm is guaranteed to avoid the problems with local minima suffered by standard ICP. In our experiments, the acquired surface data was registered to the segmented kidney model with GoICP using a change in error (RMS of closest points) stopping criteria of 0.00001 mm. Example results from each of the three surface acquisition methods are shown in Fig. 4.

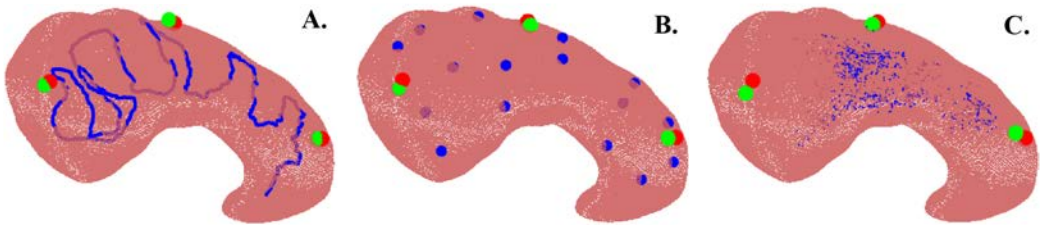

Figure 4. A visualization of the best-case results for the three surface acquisition methods. The measured target locations (i.e. pinheads) are shown in red, post-registration image space targets in green, and acquired surface data in blue): A. A kidney surface tracing with a da Vinci PSM instrument. B. Use of ink fiducial markers triangulated from stereo endoscope images. C. Use of a disparity-based point cloud generated from stereo images (stereo reconstruction).

We quantify the accuracy of our registrations by measuring the Target Registration Error (TRE)[21] associated with our surface-embedded, pinhead targets. The mean and standard deviation of these TRE measurements are reported in Table 2 for each of the surface acquisition methods and for each of the Arm Setup configurations.

Table 2. Measured TRE for each surface acquisition method considered (mean ± standard deviation, mm).

	Arm Setup 1	**Arm Setup 2**	**Arm Setup 3**
Surface Tracing with PSM Instrument Tip	5.75 ± 2.88	8.09 ± 3.23$^{\#}$	8.39 ± 3.76$^{\#}$
ECM Triangulation of Surgical Ink Fiducial Markers	6.36 ± 3.06	13.60 ± 8.53	12.16 ± 6.32
ECM Triangulation of Disparity-Based Point Cloud	5.19 ± 3.37	17.72 ± 10.19$^{\#}$	13.42 ± 4.58$^{\#}$

$\#$ indicates a significant difference ($p < 0.05$) among methods in a particular column.

We also performed a Kruskal-Wallis one-way analysis of variance test[24] on the TRE data between each of the surface acquisition methods to determine significant differences between them. For those trials in which a significant difference was found, a post-hoc Tukey's test[24] on ranks was performed to compare the accuracy of each method. Results from this analysis are reported in Table 2.

Initially, the transformations (acquired from surface registration) are only applicable to the arm in which the surface data was acquired. But in an IGS, it is useful to be able to transform points of interest into the coordinate frames of various arms. This was the reason for the final calibration process described in Section 2, in which the transformations between arm base frames were identified. The relevant coordinate frames are illustrated in Fig. 5. Since each of the base coordinate frame transformations is imperfectly known, we explored the effect on TRE of transforming points between the various frames. Table 3 illustrates these results. The rows labeled "Native" indicate the original TRE measured for the arm used for surface acquisition. The other rows give the TRE for the same set of targets points after transformation into the other two base coordinate frames.

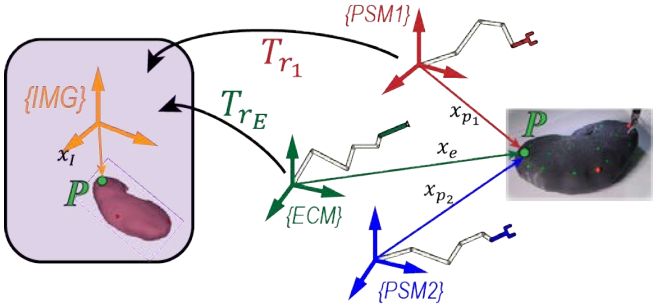

Figure 5. Each registration only initially holds for the base coordinate frame in which the surface data was acquired. However, targets in image space can be mapped into each of the three base frames by some composition of relative base frame transformations.

For each of the Arm Setup configurations and each surface acquisition method considered, a one-way analysis of variance and subsequent Tukey's test was performed to assess significant changes in TRE after transformation of image target coordinates to a non-native coordinate frame.

Table 3. Inter-frame target registration error (mean ± standard deviation, mm). Analysis of TRE measurements after image target data is transformed between calibrated (aligned) manipulator base frames.

	Frame	Arm Setup 1	Arm Setup 2	Arm Setup 3
Surface Tracing with PSM Instrument Tip	*Native*	$5.75 \pm 2.88^{\#}$	$8.09 \pm 3.23^{\#}$	$8.39 \pm 3.76^{\#}$
	PSM2	$5.61 \pm 3.68^{\dagger}$	$8.97 \pm 3.51^{\dagger}$	$8.60 \pm 4.04^{\dagger}$
	ECM	$8.99 \pm 3.51^{\#\dagger}$	$18.52 \pm 9.04^{\#\dagger}$	$17.07 \pm 5.65^{\#\dagger}$
ECM Triangulation of Surgical Ink Fiducial Markers	*Native*	$6.36 \pm 3.06^{\#\dagger}$	$13.60 \pm 8.53^{\#}$	$12.16 \pm 6.32^{\#\dagger}$
	PSM1	$11.64 \pm 2.56^{\#}$	$21.72 \pm 9.60^{\#}$	$18.10 \pm 5.26^{\#}$
	PSM2	$11.65 \pm 2.84^{\dagger}$	19.18 ± 11.12	$19.07 \pm 4.88^{\dagger}$
ECM Triangulation of Disparity-Based Point Cloud	*Native*	$5.19 \pm 3.37^{\#\dagger}$	17.72 ± 10.19	$13.42 \pm 4.58^{\#\dagger}$
	PSM1	$9.93 \pm 2.92^{\#}$	19.38 ± 6.75	$21.49 \pm 4.35^{\#}$
	PSM2	$10.24 \pm 2.35^{\dagger}$	16.55 ± 5.94	$23.41 \pm 4.54^{\dagger}$

and † indicate a significant difference in TRE ($p < 0.05$) between base frames for a given surface acquisition method and Arm Setup configuration.

A *Native* frame is that frame in which the original surface data was taken for registration where TRE measurements in these cases are the same as in Table 2.

4. DISCUSSION

In this paper, we performed several calibration processes on the da Vinci Surgical System and its endoscope and explored several potential registration procedures for the purpose of providing intraoperative image-guidance within the da Vinci console. We found that while nominal kinematic parameters yielded accurate instrument tip locations, the accuracy of our kinematic model could be significantly enhanced by calibration. Overall accuracy was comparable to the 1.02 mm previously measured by Kwartowitz et al.[22] Furthermore, we found no

significant accuracy differences for the two instruments considered (the DeBakey Forceps vs. the Black Diamond Micro Forceps).

Unsurprisingly, given the small intraocular distance of 5.4 mm between the stereo cameras in the da Vinci endoscope, localization and surface-based registration with the PSMs was more accurate than with endoscope-based techniques. However, the advantage of surface acquisition with the ECM is that it can be carried out automatically, and does not require the surgeon to pause the procedure to collect surface points with the instrument tool tip.

Furthermore, there is potential to improve endoscope localization accuracy in future work. During our experiments, we noticed that the endoscope is not held rigidly by the ECM. Rather, the ECM clamps to the trocar through which the endoscope is inserted, and there is a small tolerance between the endoscope and the inside diameter of the trocar. This allows the endoscope to translate and rotate within the trocar during robot motion. When the stereo camera's coordinate frame is moved in such a way, points triangulated with the endoscope are misrepresented with respect to the ECM's base frame. Post-hoc measurements revealed that the endoscope's tip could be displaced by as much as 4 cm and rotated by much as 5° axially during actuation (when the endoscope is positioned in worst-case configurations with respect to the trocar). Thus, it is possible to enhance the accuracy of endoscope-derived registration approaches in future studies by improving the rigidity with which the endoscope is held by the ECM trocar, or by directly tracking the endoscope pose using an external system (e.g. an optical tracker).

It is also worth noting that the hard plastic kidney phantom used in this work may have reduced registration accuracy for the surface tracing approach. During creation of the phantom, we originally viewed its rigidity as a benefit, since its geometry would be well defined, eliminating any tissue deformation effects during surface tracing. However, in practice, it was challenging for the physician to keep the tool tip in constant contact with the rigid surface without either pulling off or pushing too hard (causing instrument bending), since there is no force feedback in the da Vinci system. A qualitative visual inspection of the data leads us to believe that the surgeon likely spent much of the time hovering the instrument tip slightly above the kidney surface in our surface tracing experiments. Thus, in future work, we intend to compare registration results from soft tissue phantoms (which enable the surgeon to visually estimate applied force by observing slight tissue deformation during tracing) to our results with rigid phantoms to quantify the accuracy effects.

We also saw that the TRE measured in frame $\{PSM2\}$ given a surface tracing acquired in frame $\{PSM1\}$ was not statistically different than the measured TRE in the native frame $\{PSM1\}$. This a useful because it indicates that the surgeon may not need to separately use both arms to individually trace the kidney surface for registration, provided the relationships between manipulators' base frames have been identified. This could save time during surgery. Furthermore, in the future, instead of probing checkerboards during the alignment of base frames, it will likely be possible to automate this process with computer vision. Here, a corresponding point-set can be defined in all coordinate frames by briefly tracking instrument tool tips with the stereo endoscope before the procedure (see e.g. Zhang et al.,[32] Climent et al.,[33] or Reiter et al.[34]).

It is also worth noting that hybrid methods using manipulator surface tracing techniques and endoscope images together may become preferable to either individual approach in the future. In particular, our system may use a surface tracing to obtain a good initial registration fit, and then subsequently track features in endoscope images (e.g. using an algorithm like Puerto et al.[35] which was applied previously to monocular endoscopes but lacked an accurate initial alignment). Furthermore, it will be useful in the future to incorporate soft tissue models to predict deformed kidney shapes[11] in surgery and integrate updated shapes into our registration algorithms. Specifically, the tissue models describing tumor resection, perfusion changes, changes in urine pressure, and tool-tissue interaction[11,36] will be useful to build into our IGS. Additionally, tissue deformation could be tracked more directly in our system using endoscope images following the work of Stoyanov et al.[37] or Mountney et al.[38]

In summary, by evaluating and comparing the feasibility and accuracy of a few registration options, this paper has been a step toward a future IGS for the da Vinci Surgical System. When this image-guidance technology reaches its full potential, it is likely to have profound impacts on patient care. If it is successful in achieving our goal of increasing the utilization of partial nephrectomy in comparison to radical nephrectomy, it will dramatically improve the long-term quality of life for kidney cancer patients.

ACKNOWLEDGMENTS

This research was supported by award number R01 EB023717 from the National Institutes of Health. The content is solely the responsibility of the authors and does not necessarily represent the official views of the National Institutes of Health. The authors would like to thank Intuitive Surgical Inc. for providing the Application Programming Interface library necessary to perform this study. The authors would also like to thank Bob Galloway for many conversations that helped shape the ultimate form and content of this manuscript.

REFERENCES

[1] Herrell, S. D., Galloway, R. L., and Su, L.-M., "Image-guided robotic surgery: update on research and potential applications in urologic surgery," *Current Opinion in Urology* **22**(1), 47–54 (2012).

[2] Leven, J., Burschka, D., Kumar, R., Zhang, G., Blumenkranz, S., Dai, X. D., Awad, M., Hager, G. D., Marohn, M., Choti, M., Hasser, C., and Taylor, "DaVinci canvas: a telerobotic surgical system with integrated, robot-assisted, laparoscopic ultrasound capability," *International Conference on Medical Image Computing and Computer-Assisted Intervention*, 811–818, Springer (2005).

[3] Mohareri, O., Nir, G., Lobo, J., Savdie, R., Black, P., and Salcudean, S., "A system for MR-ultrasound guidance during robot-assisted laparoscopic radical prostatectomy," *International Conference on Medical Image Computing and Computer-Assisted Intervention*, 497–504, Springer (2015).

[4] "SEER Data, 1973-2014." seer.cancer.gov/data/. Accessed: 2017-10-30.

[5] Vogelzang, N. J. and Stadler, W. M., "Kidney cancer," *The Lancet* **352**(9141), 1691–1696 (1998).

[6] Novick, A., Campbell, S., Belldegrun, A., Blute, M., Chow, G., Derweesh, I., Faraday, M., Kaouk, J., Leveillee, R., Matinlow, S., Russo, P., and Uzzo, R., "Guideline for management of the clinical stage 1 renal mass," *Journal of Urology* **182**(4), 1271–1279 (2009).

[7] Hollenbeck, B. K., Taub, D. A., Miller, D. C., Dunn, R. L., and Wei, J. T., "National utilization trends of partial nephrectomy for renal cell carcinoma: a case of underutilization?," *Journal of Urology* **67**(2), 254–259 (2006).

[8] Kwartowitz, D. M., Miga, M. I., Herrell, S. D., and Galloway, R. L., "Towards image guided robotic surgery: multi-arm tracking through hybrid localization," *International Journal of Computer Assisted Radiology and Surgery* **4**(3), 281–286 (2009).

[9] Herrell, S. D., Kwartowitz, D. M., Milhoua, P. M., and Galloway, R. L., "Toward image guided robotic surgery: system validation," *Journal of Urology* **181**(2), 783–790 (2009).

[10] Benincasa, A. B., Clements, L. W., Herrel, S., Chang, S. S., Cookson, M. S., and Galloway, R. L., "Feasibility study for image guided kidney surgery: assessment of required intraoperative surface for accurate image to physical space registrations," *SPIE Medical Imaging* (2006).

[11] Altamar, H. O., Ong, R. E., Glisson, C. L., Viprakasit, D. P., Miga, M. I., Herrell, S. D., and Galloway, R. L., "Kidney deformation and intraprocedural registration: a study of elements of image-guided kidney surgery," *Journal of Endourology* **25**(3), 511–517 (2011).

[12] Pratt, P., Mayer, E., Vale, J., Cohen, D., Edwards, E., Darzi, A., and Yang, G.-Z., "An effective visualisation and registration system for image-guided robotic partial nephrectomy," *Journal of Robotic Surgery* **6**(1), 23–31 (2012).

[13] Su, L.-M., Vagvolgyi, B. P., Agarwal, R., Reiley, C. E., Taylor, R. H., and Hager, G. D., "Augmented reality during robot-assisted laparoscopic partial nephrectomy: toward real-time 3D-CT to stereoscopic video registration," *Journal of Urology* **73**(4), 896–900 (2009).

[14] Hamarneh, G., Amir-Khalili, A., Nosrati, M. S., Figueroa, I., Kawahara, J., Al-Alao, O., Peyrat, J.-M., Abi-Nahed, J., Al-Ansari, A., and Abugharbieh, R., "Towards multi-modal image-guided tumour identification in robot-assisted partial nephrectomy," *Middle East Conference on Biomedical Engineering*, 159–162, IEEE (2014).

[15] Schneider, C., Guerrero, J., Nguan, C., Rohling, R., and Salcudean, S., "Intra-operative pick-up ultrasound for robot assisted surgery with vessel extraction and registration: a feasibility study," *International Conference on Information Processing in Computer-Assisted Interventions*, 122–132, Springer.

[16] Hughes-Hallett, A., Mayer, E. K., Marcus, H. J., Cundy, T. P., Pratt, P. J., Darzi, A. W., and Vale, J. A., "Augmented reality partial nephrectomy: examining the current status and future perspectives," *Urology* **83**(2), 266–273 (2014).

[17] Glisson, C., Ong, R., Simpson, A., Burgner, J., Lathrop, R., Webster, R., and Galloway, R., "Registration methods for gross motion correction during image-guided kidney surgery," *International Journal of Computer Assisted Radiology and Surgery* **6**(S1), 160–161 (2011).

[18] Ong, R., Glisson, C. L., Burgner-Kahrs, J., Simpson, A., Danilchenko, A., Lathrop, R., Herrell, S. D., Webster, R. J., Miga, M., and Galloway, R. L., "A novel method for texture-mapping conoscopic surfaces for minimally invasive image-guided kidney surgery," *International Journal of Computer Assisted Radiology and Surgery* **11**(8), 1515–1526 (2016).

[19] Khalil, W. and Dombre, E., [*Modeling, identification and control of robots*], Butterworth-Heinemann (2004).

[20] Zhang, Z., "A flexible new technique for camera calibration," *IEEE Transactions on Pattern Analysis and Machine Intelligence* **22**(11), 1330–1334 (2000).

[21] Fitzpatrick, J. M., West, J. B., and Maurer, C. R., "Predicting error in rigid-body point-based registration," *IEEE Transactions on Medical Imaging* **17**(5), 694–702 (1998).

[22] Kwartowitz, D. M., Herrell, S. D., and Galloway, R. L., "Toward image-guided robotic surgery: determining intrinsic accuracy of the da vinci robot," *International Journal of Computer Assisted Radiology and Surgery* **1**(3), 157–165 (2006).

[23] DiMaio, S. and Hasser, C., "The da vinci research interface," *MICCAI Workshop on Systems and Architecture for Computer Assisted Interventions* (2008).

[24] Gibbons, J. D. and Chakraborti, S., "Nonparametric statistical inference," in [*International encyclopedia of statistical science*], 977–979, Springer (2011).

[25] Glisson, C., Ong, R., Simpson, A., Clark, P., Herrell, S., and Galloway, R., "The use of virtual fiducials in image-guided kidney surgery," *SPIE Medical Imaging* (2011).

[26] Hirschmuller, H., "Stereo processing by semiglobal matching and mutual information," *IEEE Transactions on pattern analysis and machine intelligence* **30**(2), 328–341 (2008).

[27] Vagvolgyi, B., Su, L.-M., Taylor, R., and Hager, G. D., "Video to CT registration for image overlay on solid organs," *Conference on Augmented Reality in Medical Imaging and Augmented Reality in Computer-Aided Surgery*, 78–86, Citeseer (2008).

[28] Maier-Hein, L., Mountney, P., Bartoli, A., Elhawary, H., Elson, D., Groch, A., Kolb, A., Rodrigues, M., Sorger, J., Speidel, S., and Stoyanov, D., "Optical techniques for 3D surface reconstruction in computer-assisted laparoscopic surgery," *Medical Image Analysis* **17**(8), 974–996 (2013).

[29] Pieper, S., Halle, M., and Kikinis, R., "3D slicer," *IEEE International Symposium on Biomedical Imaging*, 632–635 (2004).

[30] Cignoni, P., Callieri, M., Corsini, M., Dellepiane, M., Ganovelli, F., and Ranzuglia, G., "MeshLab: an Open-Source Mesh Processing Tool," *Eurographics Italian Chapter Conference*, The Eurographics Association (2008).

[31] Yang, J., Li, H., Campbell, D., and Jia, Y., "Go-ICP: a globally optimal solution to 3D ICP point-set registration," *IEEE transactions on pattern analysis and machine intelligence* **38**(11), 2241–2254 (2016).

[32] Zhang, X. and Payandeh, S., "Application of visual tracking for robot-assisted laparoscopic surgery," *Journal of Field Robotics* **19**(7), 315–328 (2002).

[33] Climent, J. B. and Climent, P. M., "Automatic instrument localization in laparoscopic surgery," *ELCVIA: electronic letters on computer vision and image analysis* **4**(1), 21–31 (2004).

[34] Reiter, A., Allen, P. K., and Zhao, T., "Appearance learning for 3d tracking of robotic surgical tools," *International Journal of Robotics Research* **33**(2), 342–356 (2014).

[35] Puerto-Souza, G. A., Cadeddu, J. A., and Mariottini, G.-L., "Toward long-term and accurate augmented-reality for monocular endoscopic videos," *IEEE Transactions on Biomedical Engineering* **61**(10), 2609–2620 (2014).

[36] Ong, R. E., Herrell, S. D., Miga, M. I., and Galloway, R. L., "A kidney deformation model for use in non-rigid registration during image-guided surgery," *SPIE Medical Imaging* (2008).

[37] Stoyanov, D., Mylonas, G. P., Deligianni, F., Darzi, A., and Yang, G. Z., "Soft-tissue motion tracking and structure estimation for robotic assisted mis procedures," *International Conference on Medical Image Computing and Computer-Assisted Intervention*, 139–146, Springer (2005).

[38] Mountney, P., Stoyanov, D., and Yang, G.-Z., "Three-dimensional tissue deformation recovery and tracking," *IEEE Signal Processing Magazine* **27**(4), 14–24 (2010).